A Diagnostic Indicator of the Stability of the Atlantic Meridional Overturning Circulation in CCSM3

WEI LIU AND ZHENGYU LIU

Center for Climatic Research and Department of Atmospheric and Oceanic Sciences, University of Wisconsin—Madison, Madison, Wisconsin

(Manuscript received 15 November 2011, in final form 10 September 2012)

ABSTRACT

A diagnostic indicator ΔM_{ov} is proposed in this paper to monitor the stability of the Atlantic meridional overturning circulation (AMOC). The ΔM_{ov} is a diagnostic for a basinwide salt-advection feedback and defined as the difference between the freshwater transport induced by the AMOC across the southern border of the Atlantic Ocean and the overturning liquid freshwater transport from the Arctic Ocean to the North Atlantic. As validated in the Community Climate System Model, version 3 (CCSM3), for an AMOC in the conveyor state, a positive ΔM_{ov} (freshwater convergence) in the Atlantic basin indicates a monostable AMOC and a negative ΔM_{ov} (freshwater divergence) indicates a bistable AMOC. Based on ΔM_{ov}, the authors investigate the AMOC stability in the Last Glacial Maximum (LGM) and analyze the modulation of the AMOC stability by an open/closed Bering Strait. Moreover, the authors estimate that the real AMOC is likely to be bistable in the present day, since some observations suggest a negative ΔM_{ov} (freshwater divergence) is currently in the Atlantic basin. However, this estimation is very sensitive to the choice of the observational data.

1. Introduction

The Atlantic meridional overturning circulation (AMOC) has been suggested to play a key role in rapid climate changes in the past (Clark et al. 2002; Rahmstorf 2002). The rapid change is associated with the nonlinear nature and, in turn, multiple equilibria of the AMOC. The multiple equilibria of the AMOC have been found in models of various complexity, including simple box models (Stommel 1961; Rooth 1982), ocean general circulation models (OGCMs; Bryan 1986; Marotzke et al. 1988; Marotzke and Willebrand 1991; Weaver and Sarachik 1991; Weaver and Hughes 1992; Weaver et al. 1993; Stocker and Wright 1991a,b; Power and Kleeman 1993; Zhang et al. 1993; Hughes and Weaver 1994), earth system models of intermediate complexity (EMICs; Rahmstorf et al. 2005; Hofmann and Rahmstorf 2009), and some coupled atmosphere–ocean general circulation models (AOGCMs; Manabe and Stouffer 1988; Yin and Stouffer 2007; Hawkins et al. 2011). It has, however, remained unclear if the bistable AMOC with the conveyor and collapsed states is a common characteristic of state-of-the-art AOGCMs. For example, Stouffer et al. (2006) dealt with the AMOC response to the freshwater forcing in AOGCMs of the Paleoclimate Modeling Intercomparison Project (PMIP) but found no evidence of multiple equilibria except for one AOGCM [Geophysical Fluid Dynamics Laboratory R30 (GFDL-R30); Yin and Stouffer 2007], because the AMOC restores to its original conveyor state after the termination of the freshwater hosing.

To better study the stability of the AMOC, especially in a complex climate model and in the real world, it is highly desirable to have a diagnostic indicator. In a box model, in which the Atlantic and Arctic Oceans are combined into a single box, Rahmstorf (1996) found that the meridional freshwater transport associated with the AMOC F_{OT} across the southern boundary of the Atlantic basin can be used as a diagnostic indicator for AMOC stability, with a positive F_{OT} (freshwater import) and negative F_{OT} (freshwater export) indicating a monostable regime and a bistable regime, respectively. Weber et al. (2007) further applied this indicator to PMIP climate models and found that all models except for one

Corresponding author address: W. Liu, 1225 W. Dayton St., 1143, Madison, WI 53706.
E-mail: wliu5@wisc.edu

DOI: 10.1175/JCLI-D-11-00681.1

[EMIC Climate deBilt-Coupled Large-Scale Ice Ocean (ECBilt/CLIO)] show a freshwater import across the southern border of the Atlantic basin. This is consistent with the hosing experiments of Stouffer et al. (2006), which exhibit no evidence of bistability of the AMOC in these models.

Physically, the transport indicator can be understood as follows (Rahmstorf 1996): For an AMOC of negative F_{OT} (freshwater exporting), a freshwater anomaly over the North Atlantic will reduce the AMOC and, in turn, the freshwater export. The latter will further lead to a basinwide freshening and in turn the suppression of deep convection in the North Atlantic and eventually the collapse of the AMOC. In this argument, it is clear that a better indicator should be the net convergence of the freshwater transport associated with the AMOC, with a net convergence for the monostable regime and a net divergence for the bistable regime. In general, the convergence indicator will not be the same as the transport indicator if the AMOC exchanges freshwater not only in the south with the Southern Ocean but also in the north with the Arctic. This motivates Dijkstra (2007) to modify the stability indicator as a convergence indicator Σ, which is associated with the convergence/divergence of the freshwater transport by the AMOC over the Atlantic basin. This convergence indicator has subsequently been shown valid in an OGCM coupled with an energy-balance atmosphere model (Huisman et al. 2010). However, to our knowledge, the convergence indicator has not been validated in any AOGCMs.

In this study, we propose an improved convergence indicator for the AMOC stability and for the first time validate it in a fully coupled AOGCM. As improved from Σ, our convergence indicator includes the meridional overturning freshwater transport across the Greenland, Iceland, and Norwegian (GIN) seas, since either in observation (e.g., Killworth 1983) or many AOGCMs (Schiller et al. 1997; Holland et al. 2001; Renold et al. 2010) the GIN seas are one of the major regions for the North Atlantic Deep Water (NADW) formation, and the freshwater transport via this region is very important in modulating the strength and stability of the AMOC (Holland et al. 2001; Curry and Mauritzen 2005; Komuro and Hasumi 2005; Oka and Hasumi 2006; Rennermalm et al. 2006, 2007). The remainder of the paper is structured as follows: Section 2 provides the information regarding the model and experimental design. In section 3, we propose and validate an improved AMOC stability indicator in the model. In section 4, we explore the usage of the indicator for other applications. Concluding remarks and further discussions are given in section 5.

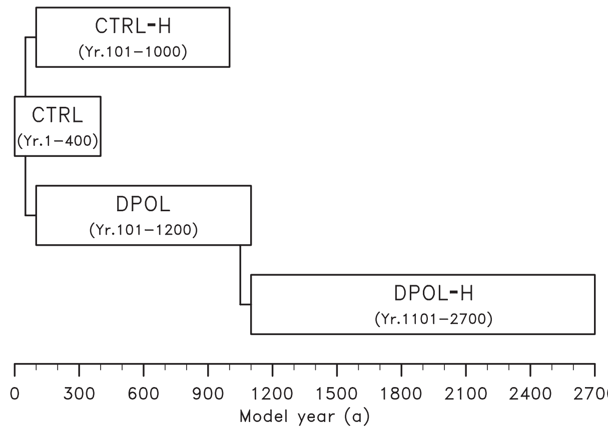

FIG. 1. Chart that illustrates the succession of experiments conducted from the CCSM3 T31_gx3v5 control run in the perpetual AD 1990 scenario. For the description of the experiments, see the main text. Specifically, CTRL is integrated for years 1–400, CTRL-H is integrated for years 101–1000, DPOL is integrated for years 101–1200, and DPOL-H is integrated for years 1101–2700.

2. Model and experiments

The AOGCM used in this study is the Community Climate System Model, version 3 (CCSM3), from the National Center for Atmospheric Research (NCAR). CCSM3 is a global, coupled ocean–atmosphere–sea ice–land surface climate model without flux adjustment (Collins et al. 2006). Unlike the EMICs, it includes a fully dynamic atmosphere model, the Community Atmosphere Model, version 2.0 (CAM2.0). All the simulations are performed in the version of T31_gx3v5 resolution (Yeager et al. 2006), which utilizes T31 spectral truncation (3.75° by 3.75° transform grid) for the atmosphere and adopts an x3ocn grid (100×116 points, nominally 3°) in the ocean and sea ice components, with 25 vertical levels in the ocean. Benefited from the x3ocn grid, the model resolution becomes significantly finer toward Greenland so that the model topography is well resolved in the Arctic and the North Atlantic. The Bering Strait is open, and the model resolution increases over the Canadian Archipelago so that it is possible to open a relatively realistic Northwest Passage between Baffin Bay and the Beaufort Sea.

The study is based on a control run of T31_gx3v5 in the perpetual AD 1990 scenario, which has been integrated for 1200 model years. By year 800, the model has reached a quasi equilibrium, except for some very slow adjustment associated with the abyssal water (Yeager et al. 2006). Thus, here, we start from year 780 (denoted here as new control year 0) and use the following 400-yr model integration as the control experiment (CTRL).

To obtain a different state from CTRL for testing the AMOC stability indicator, we conduct an experiment

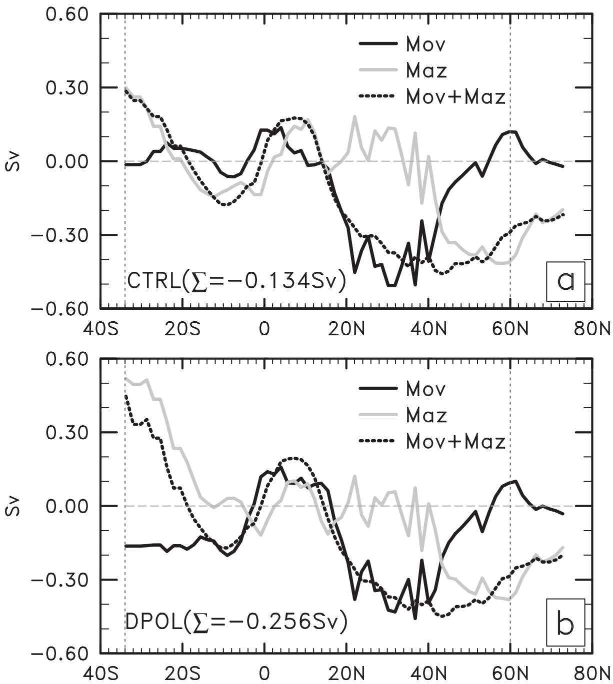

FIG. 2. The meridional freshwater transport in the Atlantic from (a) CTRL and (b) DPOL with the azimuthal component M_{az} (light gray; solid), the overturning component M_{ov} (black; solid), and the total $M_{az} + M_{ov}$ (black; dotted). The M_{az} and M_{ov} are calculated from the monthly output by Eqs. (1) and (2) and shown as a 100-yr mean (years 1–100 in CTRL and years 1001–1100 in DPOL). Here, $\Sigma = M_{ov}(60°N) - M_{ov}(34°S)$ and is calculated as -0.134 Sv in CTRL and -0.256 Sv in DPOL, respectively. The zero line is drawn as a dashed line (light gray; long dashed). The southern (34°S) and northern (60°N) boundaries of Σ are denoted as dotted lines (dark gray; dotted). In the figure, we limit M_{ov} and M_{az} to the south of around 72°N (the southernmost point of the western shelf of the Barents Sea) for strictly satisfying Eqs. (1) and (2).

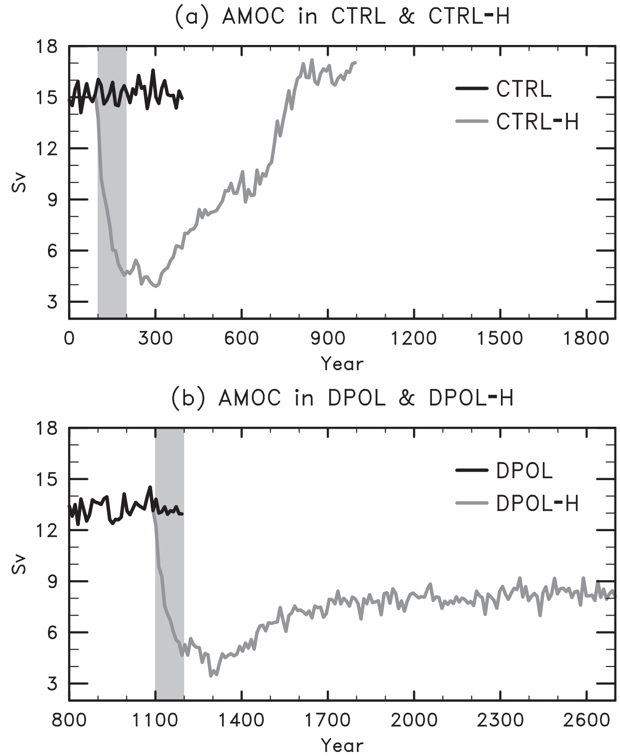

FIG. 3. Time evolution of the AMOC strength in (a) CTRL (black) and CTRL-H (dark gray) and (b) DPOL (black) and DPOL-H (dark gray). The AMOC strength is defined as the maximum streamfunction value in the circulation below 500 m within the North Atlantic basin. It is calculated from the annual mean output and shown as a decadal average. The 100-yr hosing period is shaded in light gray.

[Dipole, the experiment with a dipole-like freshwater correction (DPOL)] following the approach from De Vries and Weber (2005, hereafter, VW2005). Starting from year 100, a dipole-like freshwater correction is added into CTRL over the 17°–34°S belt in the South Atlantic gyre, with an anomalous freshwater flux of -0.25 Sv (1 Sv $\equiv 10^6$ m^3 s^{-1}) added to the west of 15°W and an anomalous freshwater flux of 0.25 Sv added to the east of 15°W. The AMOC stability in the control and DPOL climates is tested by two parallel freshwater hosing experiments (CTRL-H and DPOL-H). A 100-yr pulse of 1.0-Sv freshwater flux is uniformly distributed into the North Atlantic between 50° and 70°N from year 100 in CTRL and from year 1100 in DPOL. The freshwater flux of 1.0 Sv is approximately equal to the total runoff over the world and is sufficiently large to shut down the AMOC in many AOGCMs (Stouffer et al. 2006). Here, it should be mentioned that a 100-yr transient hosing is just a common routine for testing the AMOC stability in AOGCMs, which may not enable the model to reach a different steady state. The integration of DPOL, CTRL-H, and DPOL-H lasts 1100, 900, and 1600 yr, respectively. The experimental designs are shown in Fig. 1.

3. Results

a. The AMOC stability indicator

First, we examine the validity of the indicators F_{OT} and Σ in the CCSM3 control run. In the Atlantic, the meridional freshwater transport to the south of 72°N can be divided into two parts: the meridional overturning part M_{ov} associated with the AMOC and the azimuthally asymmetric part M_{az} associated with the wind-driven gyre circulation. These two parts are defined as

$$M_{ov} = -\frac{1}{S_0}\int dz\,\overline{v}(z)[\langle\overline{s}\rangle - S_0] \quad \text{and} \tag{1}$$

$$M_{az} = -\frac{1}{S_0}\int dz\,\overline{v'(z)s'(z)}, \tag{2}$$

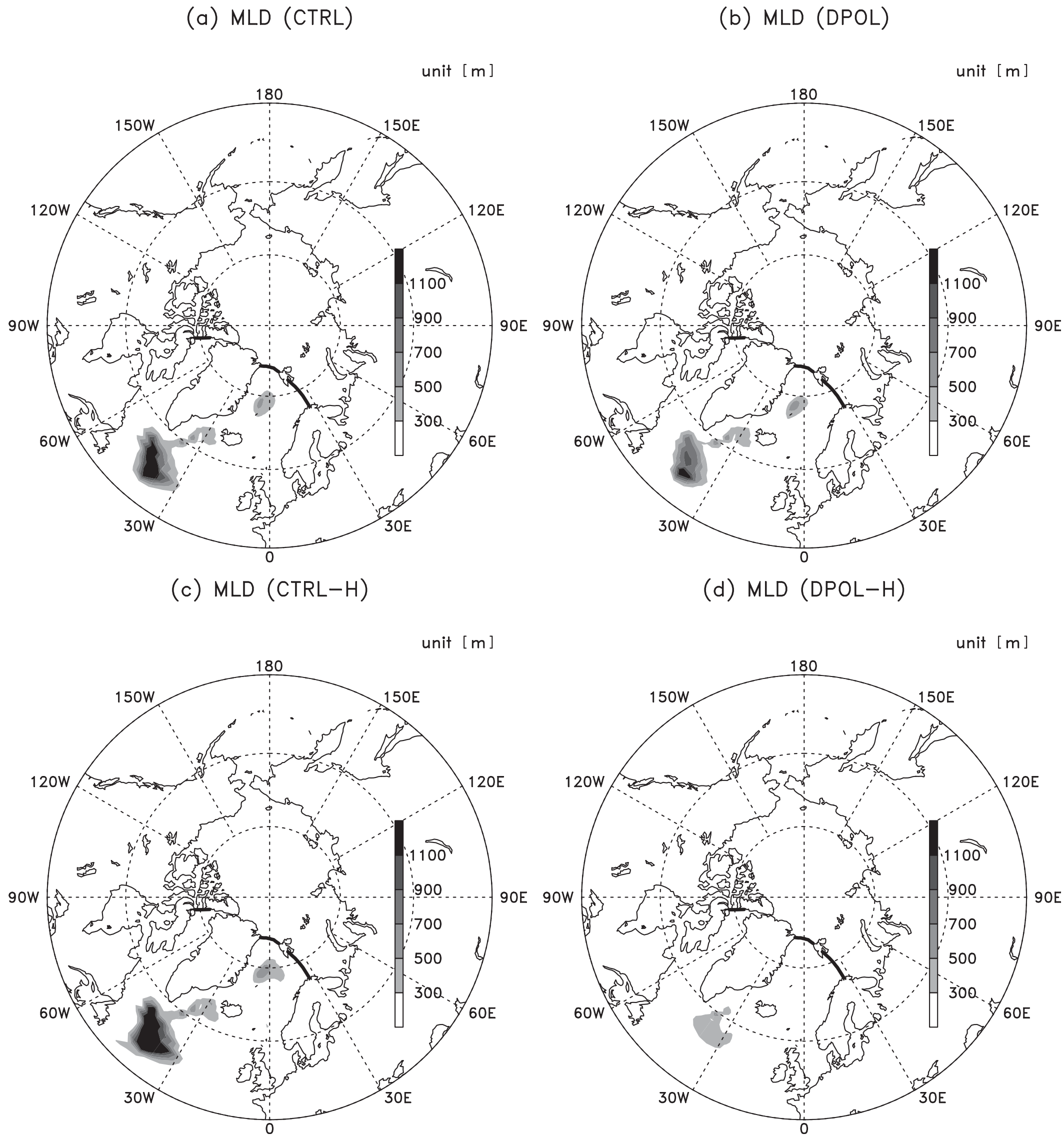

FIG. 4. The mean MLD in March over 300 m deep in (a) CTRL, (b) DPOL, (c) CTRL-H, and (d) DPOL-H. The MLD in the diagram is shown in meters and calculated as a 100-yr mean: that is, years 1–100 in CTRL, years 901–1000 in CTRL-H, years 1001–1100 in DPOL, and years 2601–2700 in DPOL-H. Three pathways of Arctic freshwater export are 1) the CAA, 2) the Fram Strait, and 3) the western shelf of the Barents Sea, whose pathways are denoted in the diagram by the thick black lines.

where S_0 is a reference salinity from a global mean value of 34.7 psu; the overbar and the angle brackets $\langle\cdot\rangle$ denote zonal integration and zonal averaging along one latitude, respectively; and v' and s' are deviations from their zonal means. Here, M_{az} and M_{ov} are calculated from the monthly output of CCSM3. Figure 2a shows the distribution of M_{ov}, M_{az}, and their sum over the Atlantic basin in the equilibrium state of the CTRL. In the figure, the AMOC in CTRL generates a freshwater export across the southern boundary of the Atlantic basin: that is, $F_{OT} = M_{ovS} = M_{ov}(34°S) = -0.014$ Sv. At the same time, it induces a northward freshwater transport across 60°N, suggesting a freshwater divergence between 34°S and 60°N of $\Sigma = M_{ov}(34°S) - M_{ov}(60°N) = -0.134$ Sv. According to Rahmstorf (1996) and Dijkstra (2007), the negative F_{OT} and Σ indicate a bistable AMOC. However, as shown in Fig. 3a, the AMOC in CTRL is in a monostable regime because the circulation rapidly recovers after the removal of the freshwater forcing. Therefore, F_{OT} and Σ do not seem to be suitable for indicating the AMOC stability in CCSM3.

To find a desirable stability indicator for the AMOC in CCSM3, we diagnose the freshwater budget integrated over a generalized Atlantic basin, which is confined to

TABLE 1. The Atlantic freshwater budget according to Eq. (3), the freshwater transport across the southern and northern boundaries of the Atlantic basin, and the AMOC strength in the four experiments. The AMOC strength Ψ is defined as the maximum in the streamfunction of the circulation below 500 m in the North Atlantic basin. All terms are shown in Sverdrups and calculated as a 100-yr mean in a steady state: that is, years 1–100 in CTRL, years 901–1000 in CTRL-H, years 1001–1100 in DPOL, and years 2601–2700 in DPOL-H. Values of ΔM_{ov}, ΔM_{ovS}, and ΔM_{ovN} in boldface emphasize the magnitude of M_{ovS} overwhelming that of M_{ovN}, changing the sign of ΔM_{ov} from positive to negative and indicating a change in AMOC stability.

Run	$[E_{\mathrm{net}}]$	M_{azS}	ΔM_{ov}	M_{ovS}	M_{ovN}	M_{azN}	Res	Ψ
CTRL	0.437	0.261	**0.112**	**−0.014**	**−0.126**	−0.019	0.045	15.0
CTRL-H	0.476	0.305	**0.119**	**−0.014**	**−0.133**	−0.024	0.028	16.4
DPOL	0.516	0.494	**−0.038**	**−0.163**	**−0.125**	−0.008	0.042	13.5
DPOL-H	0.485	0.465	**−0.015**	**−0.110**	**−0.095**	−0.001	0.034	8.2

34°S in the south and to about 80°N in the north. The northern boundary is to separate the Arctic Ocean in the north along the Canadian Arctic Archipelago (CAA), the Fram Strait, and the western shelf of the Barents Sea (Fig. 4). This extended northern boundary allows us to include all the major regions of deep-water formation within the generalized Atlantic, as indicated by the deep convection in the Labrador Sea and GIN seas. As shown in Fig. 4a, associated with deep convection in the late winter, the March mean mixed layer depth (MLD) in CTRL exceeds 1000 m in the Labrador Sea and reaches about 500 m in the GIN seas (Fig. 4a). Because of the deep convective mixing, the NADW forms in the Labrador Sea and GIN seas, making these regions the sinking sites of the AMOC. Therefore, this generalized Atlantic basin explicitly covers the AMOC pathway so that the freshwater transport across the basin is critical in regulating the AMOC stability.

The freshwater budget for the generalized Atlantic is calculated as in Eq. (3). In equilibrium, a net meridional overturning freshwater transport across the basin ΔM_{ov} is balanced by the basinwide net evaporation $[E_{\mathrm{net}}]$, the azimuthal freshwater transport at the southern M_{azS} and northern M_{azN} boundaries as well as a residual term that includes the freshwater transport by diffusion: that is,

$$[E_{\mathrm{net}}] = \Delta M_{\mathrm{ov}} + M_{\mathrm{azS}} - M_{\mathrm{azN}} + \mathrm{Res}, \qquad (3)$$

where $E_{\mathrm{net}} = E - P - R - M + B_r$. Here, the sum of evaporation is E, precipitation is P, runoff is R, sea ice melting is M, brine rejection from sea ice melting is B_r, and $[\cdot]$ denotes a basinwide averaging.

The net meridional overturning freshwater transport ΔM_{ov} in Eq. (3) is defined as

$$\Delta M_{\mathrm{ov}} = M_{\mathrm{ovS}} - M_{\mathrm{ovN}}, \qquad (4)$$

where M_{ovS} and M_{ovN} are the meridional overturning freshwater transports across the southern and northern boundaries of the Atlantic basin, respectively, and M_{ovN} is equal to the overturning component of liquid freshwater import from the Arctic Ocean. Previous studies (e.g., Aagaard and Carmack 1989; Serreze et al. 2006; Holland et al. 2007; Jahn et al. 2010) show that the liquid Arctic freshwater enters the North Atlantic through three sections: the CAA, the Fram Strait, and the western shelf of the Barents Sea. Thus,

$$M_{\mathrm{ovN}} = M_{\mathrm{ovCAA}} + M_{\mathrm{ovFRA}} + M_{\mathrm{ovBAR}} \quad \text{and} \qquad (5)$$

$$M_{\mathrm{azN}} = M_{\mathrm{azCAA}} + M_{\mathrm{azFRA}} + M_{\mathrm{azBAR}}, \qquad (6)$$

where M_{ovCAA}, M_{ovFRA}, and M_{ovBAR} (M_{azCAA}, M_{azFRA}, and M_{azBAR}) are the overturning (azimuthal) liquid freshwater transports across the CAA, the Fram Strait, and the western shelf of the Barents Sea, respectively. Calculation of M_{ovCAA}, M_{ovFRA}, M_{ovBAR}, M_{azCAA}, M_{azFRA}, and M_{azBAR} generally follows Eqs. (1) and (2), in which $\bar{v}$ and v' are normal to the section while integration and averaging are along the direction of section (Fig. 4). It is worth mentioning that, besides M_{ovN}, the azimuthal component M_{azN} also contributes to the Arctic freshwater sinks into the Atlantic, but with a much smaller partition (Table 1). For example, at the Fram Strait, the northward West Spitsbergen Current carries a warm and saline water into the Arctic Ocean while the southward East Greenland Current induces fresh Arctic water to the GIN seas in the surface layer (e.g., Aagaard and Carmack 1989; Serreze et al. 2006), so that this azimuthally asymmetric pattern leads to a liquid freshwater transport from the Arctic to the North Atlantic. Also, besides the liquid Arctic freshwater, a substantial amount of ice enters the North Atlantic via the Fram Strait, which has an input of freshwater in the North Atlantic and modulates the sea ice melting and the sea ice formation in the North Atlantic. This effect has been included in the surface flux $[E_{\mathrm{net}}]$ by terms M and B_r.

We propose ΔM_{ov} as an improved convergence indicator of the AMOC stability for CCSM3 because it contains the full mechanism of the basin-scale salt-advection feedback (Stommel 1961) in this AOGCM. Consider the AMOC in its conveyer state; a freshwater discharge will weaken the AMOC. If ΔM_{ov} is positive (freshwater convergence), the initial weakening of the AMOC will reduce the freshwater convergence and therefore salinify the ocean, which then promotes deep mixing and in turn prevents a further weakening of the AMOC. Alternatively, the initial weakening of the AMOC will be amplified if ΔM_{ov} is negative. This is because the initial weakening of the AMOC reduces the divergence of the freshwater and therefore promotes a freshwater accumulation in the basin, which tends to suppress deep convection and therefore further amplify the initial weakening of the AMOC.

b. *Validation of the indicator*

To test the convergence indicator ΔM_{ov}, we first conduct a DPOL experiment following VW2005 (see section 2). In the experiment, a dipole-like freshwater correction applies over the South Atlantic. This freshwater flux correction increases the longitudinal salinity contrast at the southern border of the Atlantic basin. The Brazil Current transports much saltier water southward, and the Benguela Current transports much fresher water northward (Fig. 5), resulting in an increase of the azimuthal freshwater transport M_{azS} (Figs. 6b, 7d). At the same time, the Brazil Current has an eastward branch around 34°S, carrying much saltier surface and thermocline waters away from the west of the southern American continent (Fig. 5). As a result, the zonal mean salinity is largely enhanced (Fig. 6a). The "excess" salt flows out via the strong southward Brazil Current, which results in an enhanced freshwater export in the upper limb of the AMOC. Meanwhile, the deep southward-flowing NADW is mildly freshened, which leads to a small reduction in the freshwater export by the lower limb of the AMOC. With the combination of these two limbs, the AMOC produces a much stronger freshwater export M_{ovS} in DPOL than in CTRL (Fig. 6c).

Figure 7 displays the evolution of the AMOC and its associated freshwater transport, as well as the components in a basinwide freshwater budget during the adjustment from CTRL to DPOL. The azimuthal component M_{azS} and net evaporation $[E_{net}]$ are directly related to the rapid adjustments in the atmosphere and upper ocean as well as the interfacial atmosphere–ocean coupling, so that they enhance soon after the input of the freshwater correction and then keep steady within the whole integration period. The overturning component M_{ovS} is associated with the relatively slow adjustment of the AMOC in which the circulation strength has a reduction of 4 Sv in the first 300 yr and then gradually recovers back to 13.5 Sv by year 1200. The input freshwater flux correction is confined within the belt of 17°–34°S. Therefore, it mainly modifies the salinity structure to the south of 10°N via the wind-driven gyre

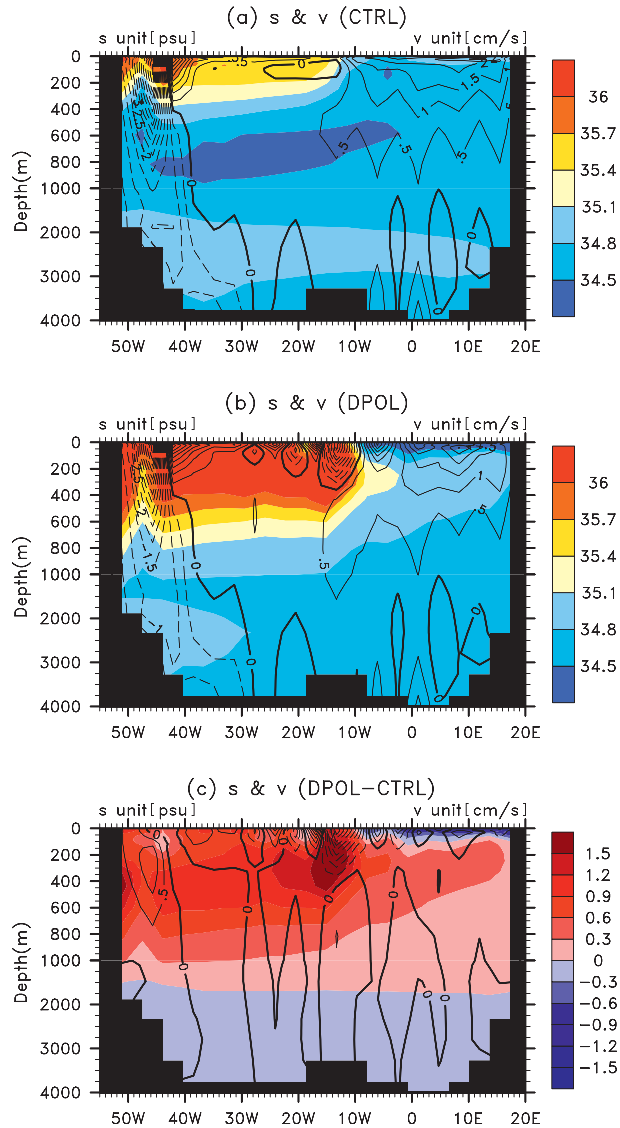

FIG. 5. Salinity (shaded; psu) and meridional velocity (contoured; cm s^{-1}) at 34°S in (a) CTRL and (b) DPOL, as well as (c) the difference between these two experiments. Salinity and meridional velocity are calculated as a 100-yr mean: that is, years 1–100 in CTRL and years 1001–1100 in DPOL. In each plot, the upper 1000 m are amplified.

circulation in the southern Atlantic and equatorial regions (Fig. 8g) and therefore changes the overturning freshwater transports in the north (M_{ovCAA}, M_{ovFRA}, and M_{ovBAR}) only slightly. In contrast, the freshwater export M_{ovS} increases significantly after the freshwater flux correction. As a result, the freshwater export M_{ovS} exceeds the freshwater import M_{ovN} after about year 500 (Fig. 7c), generating a freshwater divergence ($\Delta M_{ov} < 0$) in the Atlantic basin.

Table 1 summarizes the Atlantic freshwater budget, associated freshwater transports, and the AMOC strength

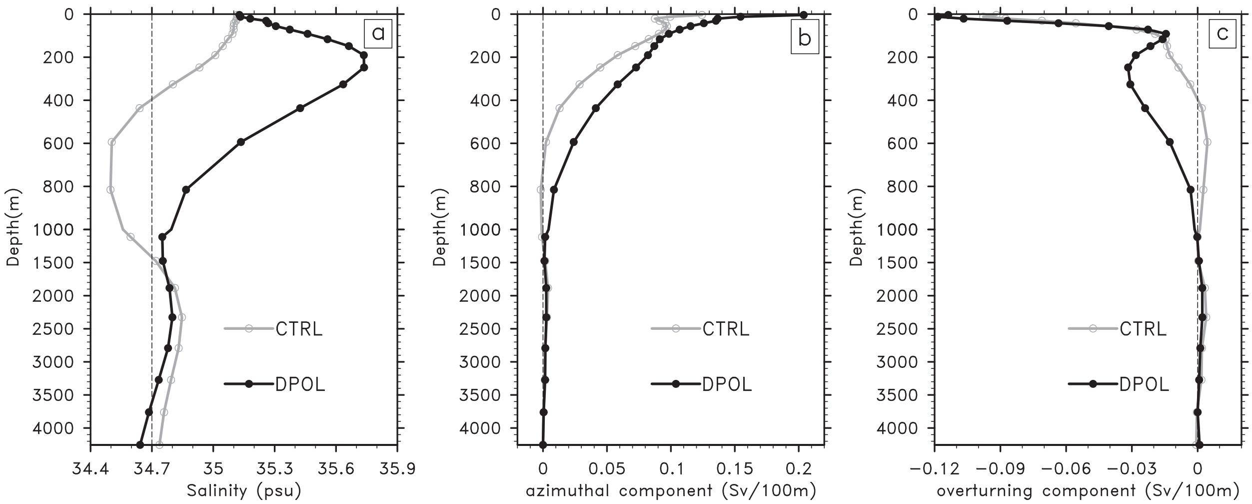

FIG. 6. (a) Zonal mean salinity, (b) the azimuthal component, and (c) the overturning component at 34°S as a function of depth in CTRL (light gray) and DPOL (black). For the values in (b) and (c) [Sv (100 m)$^{-1}$], vertical integrations equal the M_{az} and M_{ov} in Eqs. (1) and (2). Each profile in the figure is calculated as a 100-yr mean: that is, years 1–100 in CTRL and years 1001–1100 in DPOL. In each plot, the upper 1000 m are amplified.

in the equilibrium state of four experiments. The AMOC strength here is defined as the maximum in the streamfunction of the circulation below 500 m in the North Atlantic basin. From the table, a dipole-like freshwater flux correction slightly changes the AMOC strength (from 15.0 to 13.5 Sv) but significantly modulates the Atlantic freshwater budget. The azimuthal freshwater transport M_{azS} is greatly enhanced to balance most of the net evaporation $[E_{net}]$ in the basin. More importantly, the net meridional overturning freshwater transport ΔM_{ov} switches from a convergence of 0.112 Sv in CTRL to a divergence of -0.038 Sv in DPOL, which indicates a transition of the AMOC stability from a monostable regime in CTRL to a bistable regime in DPOL.

We test the diagnostic indicator ΔM_{ov} by means of the two parallel freshwater hosing experiments (CTRL-H and DPOL-H). From the steady state in CTRL (DPOL), we impose a strong pulse of freshwater perturbation to test the AMOC stability in this state. As shown in Fig. 3, the AMOCs in CTRL-H and DPOL-H are shut down during the 100-yr hosing period. However, the cease of the AMOC in CTRL-H causes a net salinifying effect in the Atlantic basin. The excess salinity gets evolved in restarting the deep convection in the Labrador Sea and GIN seas (Figs. 9a,c, 4c). As a result, the AMOC rapidly recovers 600 yr after the termination of the freshwater perturbation (Fig. 3). The experiment CTRL-H is therefore consistent with a freshwater convergence ($\Delta M_{ov} > 0$) for a monostable AMOC.

On the other hand, the collapse of the AMOC in DPOL-H induces a net freshening effect in the Atlantic basin. The excessive freshwater accumulates in the upper 400 m in the North Atlantic (Fig. 8d), especially between 40° and 80°N (Fig. 10f), to stabilize the stratification in the Labrador Sea and GIN seas. As a result, deep convection is inhibited in the GIN seas, with a mean MLD shallower than 100 m in the late winter (Fig. 9b). Meanwhile, deep convection is also greatly suppressed in the Labrador Sea, with a March mean MLD reducing from 900 m in the prehosing period to 300 m in the posthosing period (Fig. 9b). The remaining deep convective mixing in the Labrador Sea can only induce a very limited NADW formation (Fig. 8d). As a result, the AMOC, instead of recovering, resides in a weak stable state after the termination of the freshwater perturbation. The experiment DPOL-H proves that a freshwater divergence ($\Delta M_{ov} < 0$) indicates a bistable AMOC.

4. Implications

a. *The stability of real-world AMOC at the present day*

An important usage of the AMOC stability indicator is to estimate the stability of the AMOC in the real world from the observations. Previous studies (Huisman et al. 2010; Hawkins et al. 2011) that are based on F_{OT} suggest a potential existence of a bistable AMOC in the present day since most observations and reanalysis data (Weijer et al. 1999; Huisman et al. 2010; Hawkins et al. 2011) consistently support a negative F_{OT}, in the form of M_{ovS}, induced by the AMOC across the southern border of the Atlantic basin.

In this study, we estimate the present-day AMOC stability based on the indicator ΔM_{ov}. From the observations,

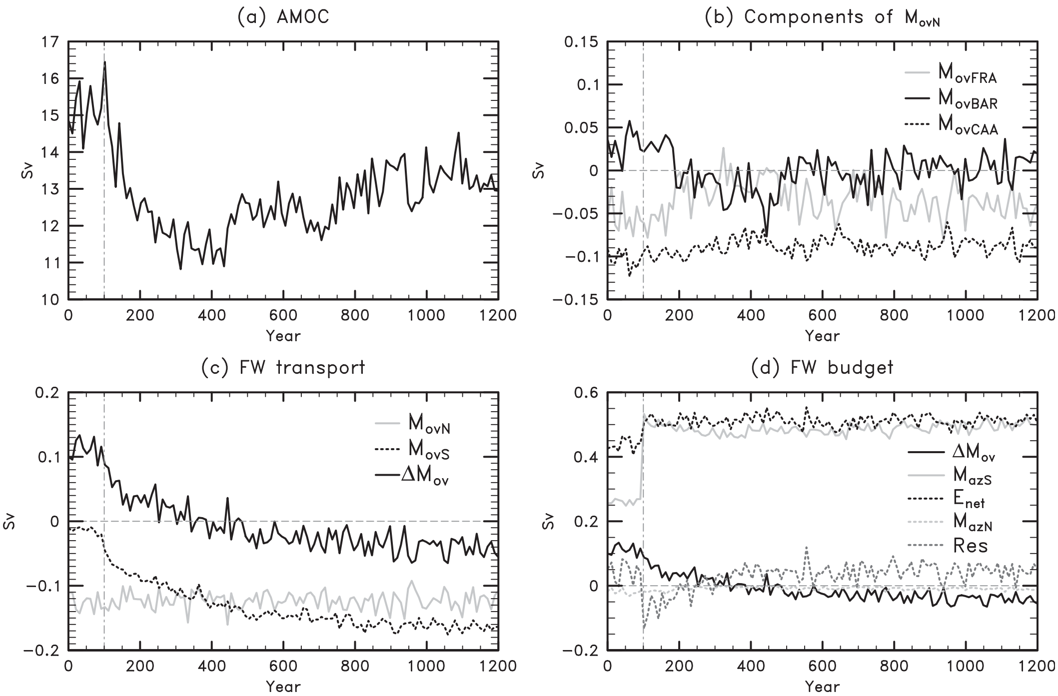

FIG. 7. Time evolution of (a) the AMOC strength; (b) the overturning liquid freshwater transport through the CAA, the Fram Strait, and the western shelf of the Barents Sea [i.e., M_{ovCAA} (black; dotted), M_{ovFRA} (light gray; solid) and M_{ovBAR} (black; solid)]; (c) the overturning freshwater transport across the southern and northern boundaries [i.e., M_{ovS} (black; dotted) and M_{ovN} (light gray; solid)], as well as the net freshwater transport in the Atlantic basin ΔM_{ov} (black; solid) as induced by the AMOC; and (d) components of the freshwater budget: the basinwide net evaporation [E_{net}] (black; dotted), the net overturning freshwater transport across the basin ΔM_{ov} (black; solid), the azimuthal freshwater transport at 34°S M_{azS} (light gray; solid), the azimuthal freshwater transport at the northern boundary of the Atlantic basin M_{azN} (light gray; dotted), and the residual Res (dark gray; dotted) during the integration of DPOL. The AMOC strength is calculated from the annual mean output and shown as a decadal mean. All freshwater transports and the net evaporation are calculated from the monthly output and shown in decadal means.

Weijer et al. (1999) find that the AMOC is associated with a 0.2-Sv freshwater export across the southern border of the Atlantic: that is, $M_{ovS} = -0.2$ Sv. In the meantime, Serreze et al. (2006) report that, associated with the present-day AMOC, the liquid Arctic freshwater enters the North Atlantic with 2660 km^3 yr^{-1} via the Fram Strait, 110 km^3 yr^{-1} via the Barents Sea, and 3200 km^3 yr^{-1} via the CAA, which gives a total Arctic freshwater transport of 5970 km^3 yr^{-1} (0.189 Sv) into the North Atlantic. As discussed in section 3, the total liquid Arctic freshwater transport is accomplished by its azimuthal and overturning components so that $M_{ovN} > -0.189$ Sv. Therefore, the present-day AMOC is estimated to generate a freshwater divergence ($\Delta M_{ov} < 0$) across the Atlantic basin, which indicates that the circulation is in a bistable regime, consistent with the transport indicator F_{OT}.

However, this estimation has a great uncertainty. First, M_{ovS} and M_{ovN} adopted in the estimation are based on different reference salinities (M_{ovS} based on 35.08 psu and M_{ovN} based on 34.8 psu). The ΔM_{ov} is prone to be modified if a uniform reference salinity is applied in the calculation of M_{ovS} and M_{ovN}. Second, M_{ovS} (and, in turn, ΔM_{ov}) has a great uncertainty as it is calculated from different observational data. For example, Huisman et al. (2010) propose a 0.1-Sv freshwater export of the AMOC across the southern boundary ($M_{ovS} = -0.1$ Sv) by using different observational data from Weijer et al. (1999). Hawkins et al. (2011) report that M_{ovS} is generally negative in multiple ocean reanalysis data, but with large variations in magnitude, ranging from close to zero to over -0.2 Sv. Therefore, based on these studies, the net freshwater transport may be either convergent or divergent in the Atlantic basin so that the present-day AMOC is either monostable or bistable.

b. ΔM_{ov} and the AMOC stability in the LGM

Besides the present-day scenario, the indicator ΔM_{ov} can also correctly indicate the AMOC stability in the Last Glacial Maximum (LGM) scenario. From a recent simulation of transient climate evolution of the last 21.0 thousand years [ka; Transient Climate Evolution of the

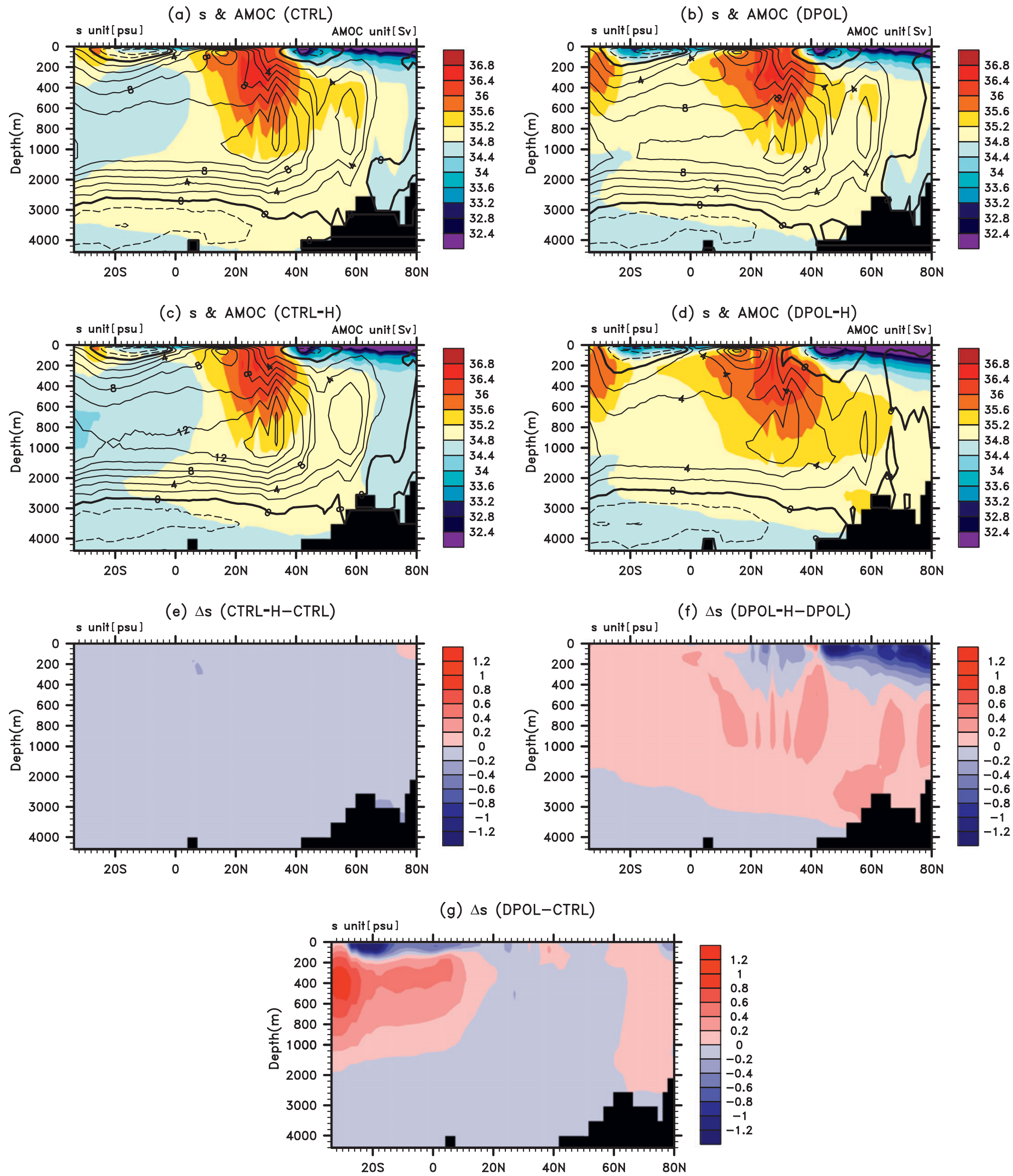

FIG. 8. Atlantic overturning streamfunction (contoured; Sv) and Atlantic zonal mean salinity (shaded; psu) in (a) CTRL, (b) DPOL (c) CTRL-H, and (d) DPOL-H, as well as Atlantic zonal mean salinity differences (shaded; psu) (e) between CTRL-H and CTRL, (f) between DPOL-H and DPOL, and (g) between DPOL and CTRL. Streamfunction and salinity are calculated by a 100-yr averaging: that is, years 1–100 in CTRL, years 901–1000 in CTRL-H, years 1001–1100 in DPOL, and years 2601–2700 in DPOL-H. In each plot, the upper 1000 m are amplified.

Last 21 000 years (TraCE-21000); Liu et al. 2009; He 2011], we calculate that the global mean salinity equals 36.5 psu during the LGM (19.0 ka Before Present). Based on $S_0 = 36.5$ psu, we find a freshwater convergence of 0.202 Sv across the Atlantic basin ($\Delta M_{ov} = 0.202$ Sv). This positive ΔM_{ov} indicates a monostable LGM AMOC, which has been demonstrated in Liu et al. (2009) and He (2011).

c. *Role of the Bering Strait*

The opening of the Bering Strait plays an important role in regulating the AMOC stability (De Boer and Nof 2004a,b), which can be explained by ΔM_{ov} since it connects the Arctic freshwater budget with the AMOC stability. In the present-day scenario, a closed Bering Strait cuts off the import of low-salinity water from the North

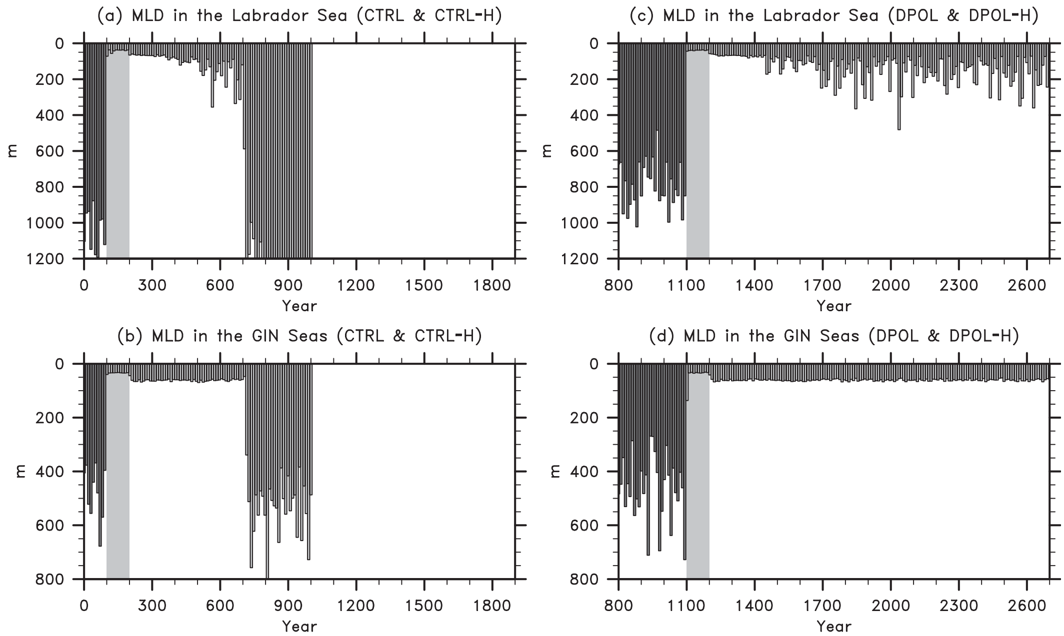

FIG. 9. (top) Time evolution of the mean MLD in March averaged in the Labrador Sea area (50°–55°N, 45°–35°W). (bottom) Time evolution of the mean MLD in March averaged in the GIN seas area (72°–75°N, 8°–2°W). (a),(b) The MLD is from CTRL during years 1–100 and from CTRL-H during years 101–1000. (c),(d) The MLD is from DPOL during years 801–1100 and from DPOL-H during years 1101–2700. MLD in each plot is calculated as a decadal mean. The 100-yr hosing period is shaded in light gray.

Pacific, which modulates the freshwater budget over the Arctic Ocean (Hu and Meehl 2005; Hu et al. 2007) and leads to a decreasing liquid Arctic freshwater export (Hu et al. 2008). Correspondingly, the magnitude of M_{ovN} is reduced. Therefore, in terms of M_{ovN}, a reduction in M_{ovN} caused by a closed Bering Strait contributes an analogous divergence to ΔM_{ov}, which tends to make the AMOC shift from a monostable regime toward a bistable regime.

5. Conclusions and discussion

In this paper, we propose an improved AMOC stability indicator ΔM_{ov}, which is defined as the difference between the freshwater transport M_{ovS} induced by the AMOC across the southern border of the Atlantic and the overturning liquid freshwater transport M_{ovN} from the Arctic to the North Atlantic. The ΔM_{ov} is a diagnostic for the basinwide salt-advection feedback. Compared with previous indicators, ΔM_{ov} accurately indicates the AMOC stability in CCSM3, either for a monostable regime (CTRL) or a bistable regime (DPOL). In CTRL, a freshwater convergence ($\Delta M_{\mathrm{ov}} > 0$) is induced by the AMOC in the Atlantic basin, which indicates a monostable circulation. In DPOL, the AMOC generates a freshwater divergence ($\Delta M_{\mathrm{ov}} < 0$) in the Atlantic, and the circulation is within a bistable regime.

This improved indicator ΔM_{ov} can also be applied to diagnose the AMOC stability in other studies. In TraCE-21000, ΔM_{ov} correctly indicates a monostable AMOC in the LGM. Besides, in the present-day scenario, ΔM_{ov} tends to be more divergent with a closed Bering Strait, which induces a shift of the AMOC stability toward a bistable regime. It is worth mentioning that the opening of the Bering Strait is one of the essential deglacial processes in the paleoclimate studies (e.g., De Boer and Nof 2004a,b; He 2011); a thorough investigation of ΔM_{ov} will shed light on the evolution of the AMOC stability during the last deglaciation.

More importantly, we estimate the AMOC stability for the real world based on observations. The AMOC is likely to be bistable in the present day, as indicated by a freshwater divergence ($\Delta M_{\mathrm{ov}} < 0$) in the Atlantic basin. However, this estimation is very sensitive to the choice of the observational data. Compared with other indicators, ΔM_{ov} includes the contribution from M_{ovN}, which make the estimation of a bistable present-day AMOC less robust.

In the following, we would like to discuss several associated issues. First, unlike the observation-based estimation, most state-of-the-art AOGCMs can only simulate a monostable AMOC in a preindustrial scenario. As we speculate, this is because M_{ovS} is generally negative (Weber et al. 2007; Drijfhout et al. 2010) and in turn ΔM_{ov}

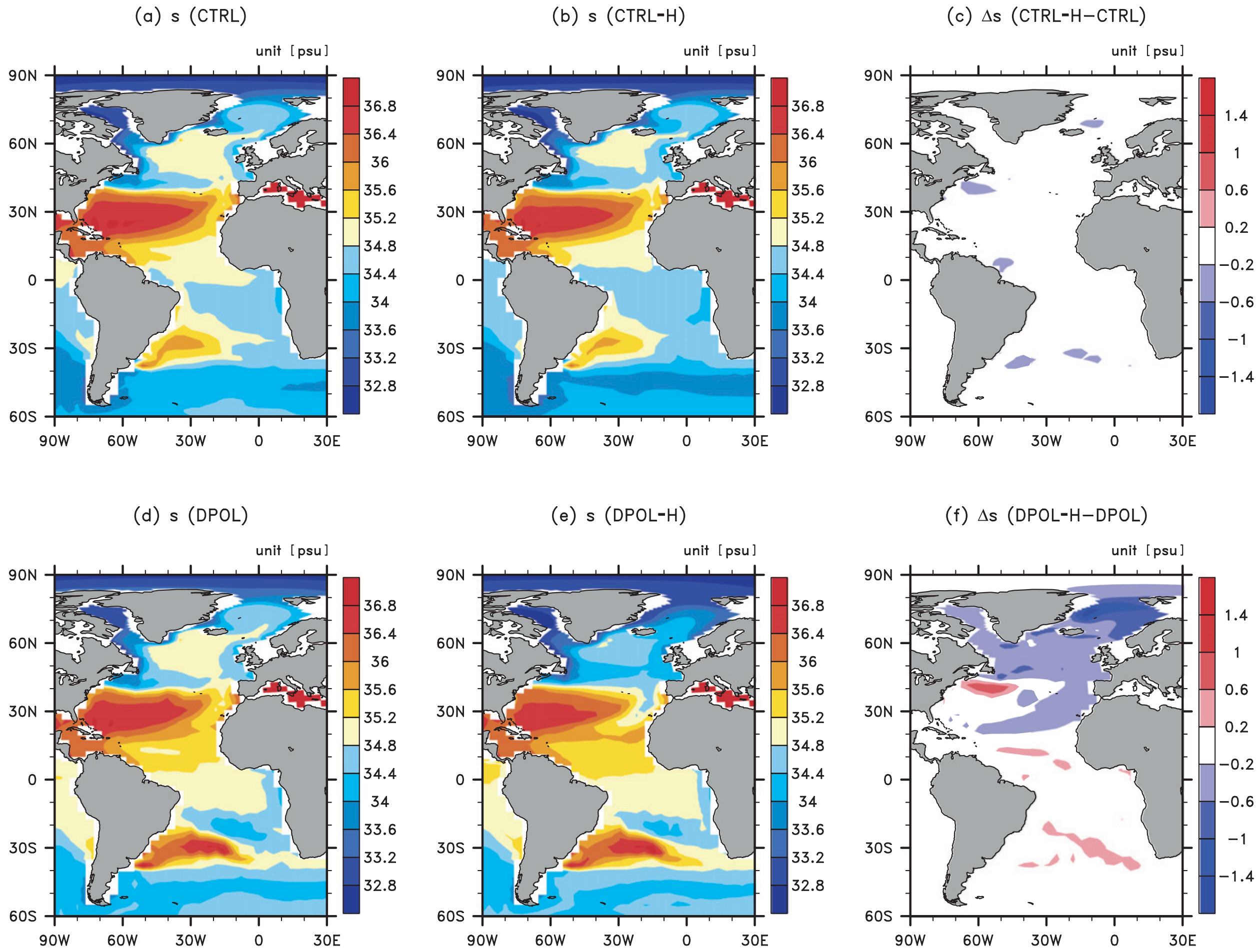

FIG. 10. (top) Maps of the average salinity in the upper 400 m from (a) CTRL and (b) CTRL-H as well as (c) the salinity differences between CTRL-H and CTRL. (bottom) Maps of the average salinity in the upper 400 m from (d) DPOL and (e) DPOL-H as well as (f) the salinity differences between DPOL-H and DPOL. Salinity (psu) is calculated as a 100-yr mean in a steady state: that is, years 1–100 in CTRL, years 901–1000 in CTRL-H, years 1001–1100 in DPOL, and years 2601–2700 in DPOL-H.

is positive (a freshwater convergence) in these models. Compared with observations, most AOGCMs simulate much fresher surface and thermocline waters but a slightly saltier NADW around 34°S, which leads to a freshwater import ($M_{ovS} > 0$, as in all the AOGCMs from PMIP) or a very weak freshwater export ($M_{ovS} < 0$, as in CTRL from this study) induced by the AMOC across the southern border of the Atlantic. Meanwhile, a strong freshwater import M_{ovN} comes from the Arctic. Therefore, a freshwater convergence is generated within the Atlantic basin by the cooperation between M_{ovN} and M_{ovS} or a dominant contribution from M_{ovN}, which results in a monostable AMOC in these AOGCMs. In our future work, we will focus on correcting the ΔM_{ov} in CCSM3 toward an observational value, for a realistic simulation of the AMOC in the present day.

Second, it is worth mentioning that ΔM_{ov} indeed indicates a basin-scale freshwater feedback associated with the NADW cell so that it may not be valid when the Antarctic Intermediate Water (AAIW) reverse cell has a strong effect on the Atlantic freshwater budget. As shown in section 3, ΔM_{ov} is valid in this study because the collapsed state of the AMOC behaves as a very weak NADW cell, and the bistability of the AMOC is primarily determined by a basin-scale salinity advection related to the NADW cell (Fig. 8). On the other hand, several studies (e.g., Saenko et al. 2003; Gregory et al. 2003; Sijp and England 2006; Sijp et al. 2012) suggested that, for a bistable AMOC, the collapsed circulation appears as an AAIW reverse cell, and the nonlinear behavior of the AAIW reverse cell plays a critical role in suppressing the NADW formation and maintaining the collapsed state (Sijp et al. 2012). Therefore, we speculate that the indicator ΔM_{ov} may not be applicable to the AMOC in these studies.

Third, we should point out that we utilize a constant salinity S_0 rather than the 34°S section-average salinity

S_m [$S_m = \int_{34°S} dz(\bar{s})/\int_{34°S} dz(1)$] as the reference salinity in the calculation of M_{ov}. This is because the usage of S_m can only guarantee a correct removal of the barotropic contribution in M_{ov} at the southern boundary of the Atlantic (Drijfhout et al. 2010) but not at the northern boundary as well. Hence, it is unsuitable to use S_m for calculating the convergence indicator ΔM_{ov} in our study. On the other hand, by choosing a constant S_0, which is close to the basin-averaged salinity over the Atlantic Ocean, we can make sure that the barotropic transports across the southern and northern boundaries of the Atlantic mostly cancel with each other. As a result, ΔM_{ov} has little contribution from the barotropic transport, which enables it to correctly represent the net meridional overturning freshwater transport across the Atlantic basin.

Actually, the barotropic transport induced by S_0 does not change our conclusion in section 3a. At 34°S, $S_m = 34.767$ psu in CTRL and $S_m = 34.883$ psu in DPOL, which are both very close to S_0. Based on S_m, we calculate that $M_{ovS} = -0.011$ Sv in CTRL and $M_{ovS} = -0.168$ Sv in DPOL, which suggests that the barotropic transport induced by S_0 only slightly modifies M_{ovS} in magnitude but does not change the sign of M_{ovS} (Table 1). As a result, the transport indicator is still negative, incorrectly indicating the AMOC in CTRL.

Finally, we must clarify that the hosing experiment adopted in this study is a commonly used and perhaps, a currently applicable way to study the AMOC stability in state-of-art AOGCMs. Unlike simple models (Stommel 1961; Rooth 1982; Tziperman et al. 1994; Rahmstorf 1996), the complexity of AOGCMs does not allow us to calculate the analytical solutions of the AMOC and obtain all the unstable modes (multiple equilibria) of the circulation by means of stability analysis. Thus, for AOGCMs, a practical way to find the unstable modes of the AMOC is to add a perturbation and see which state the model will reside in. Among various perturbations, we choose one that is more physically plausible: the freshwater perturbation in the high latitude of the North Atlantic (also named the hosing experiment) to test the AMOC stability. This added freshwater perturbation follows the physical concept of Rahmstorf (1996), and helps us to get a seeming ''optimal'' unstable mode of the AMOC in the complex AOGCMs. The resulting unstable mode of the AMOC is associated with a basin-scale salinity-advection feedback (Stommel 1961), which is different from the convective instability in Lenderink and Haarsma (1994).

Acknowledgments. The authors gratefully acknowledge Feng He, Jun Cheng, Aixue Hu, and Alexandra Jahn for useful suggestions and discussion. The authors also sincerely thank Eli Tziperman and two other analogous reviewers for their illustrating and helpful comments on the early version of this paper. The work is supported by the Priority Academic Program Development of Jiangsu Higher Education Institutions (PAPD). Also, U.S. NSF and Chinese NSF: NSFC 41130105.

REFERENCES

Aagaard, K., and E. C. Carmack, 1989: The role of sea ice and other fresh water in the Arctic Circulation. *J. Geophys. Res.,* **94,** 14 485–14 498.

Bryan, F., 1986: High-latitude salinity effects and interhemispheric thermohaline circulations. *Nature,* **323,** 301–304.

Clark, P. U., N. G. Pisias, T. F. Stocker, and A. J. Weaver, 2002: The role of the thermohaline circulation in abrupt climate change. *Nature,* **415,** 863–869.

Collins, W. D., and Coauthors, 2006: The Community Climate System Model Version 3 (CCSM3). *J. Climate,* **19,** 2122–2143.

Curry, R., and C. Mauritzen, 2005: Dilution of the northern North Atlantic Ocean in recent decades. *Science,* **308,** 1772–1774.

De Boer, A. M., and D. Nof, 2004a: The exhaust valve of the North Atlantic. *J. Climate,* **17,** 417–422.

——, and ——, 2004b: The Bering Strait's grip on the Northern Hemisphere climate. *Deep-Sea Res. I,* **51,** 1347–1366.

De Vries, P., and S. L. Weber, 2005: The Atlantic freshwater budget as a diagnostic for the existence of a stable shut down of the meridional overturning circulation. *Geophys. Res. Lett.,* **32,** L09606, doi:10.1029/2004GL021450.

Dijkstra, H. A., 2007: Characterization of the multiple equilibria regime in a global ocean model. *Tellus,* **59A,** 695–705.

Drijfhout, S. S., S. L. Weber, and E. van der Swalow, 2010: The stability of the MOC as diagnosed from model projections for pre-industrial, present and future climates. *Climate Dyn.,* **37,** 1575–1586, doi:10.1007/s00382-010-0930-z.

Gregory, J. M., O. A. Saenko, and A. J. Weaver, 2003: The role of the Atlantic freshwater balance in the hyteresis of the meridional overturning circulation. *Climate Dyn.,* **21,** 707–717, doi:10.1007/s00382-003-0359-8.

Hawkins, E., R. S. Smith, L. C. Allison, J. M. Gregory, T. J. Woollings, H. Pohlmann, and B. de Cuevas, 2011: Bistability of the Atlantic overturning circulation in a global climate model and links to ocean freshwater transport. *Geophys. Res. Lett.,* **38,** L10605, doi:10.1029/2011GL047208.

He, F., 2011: Simulating transient climate evolution of the last deglaciation with CCSM3. Ph.D. thesis, University of Wisconsin—Madison, 171 pp.

Hofmann, M., and S. Rahmstorf, 2009: On the stability of the Atlantic meridional overturning circulation. *Proc. Natl. Acad. Sci. USA,* **106,** 20 584–20 589.

Holland, M. M., C. M. Bitz, M. Eby, and A. J. Weaver, 2001: The role of ice–ocean interactions in the variability of the North Atlantic thermohaline circulation. *J. Climate,* **14,** 656–675.

——, J. Finnis, A. P. Barrett, and M. C. Serreze, 2007: Projected changes in Arctic Ocean freshwater budgets. *J. Geophys. Res.,* **112,** G04S55, doi:10.1029/2006JG000354.

Hu, A., and G. A. Meehl, 2005: Bering Strait throughflow and the thermohaline circulation. *Geophys. Res. Lett.,* **32,** L24610, doi:10.1029/2005GL024424.

——, ——, and W. Han, 2007: Role of the Bering Strait in the thermohaline circulation and abrupt climate change. *Geophys. Res. Lett.,* **34,** L05704, doi:10.1029/2006GL028906.

——, B. L. Otto-Bliesner, G. A. Meehl, W. Han, C. Morrill, E. C. Brady, and B. Briegleb, 2008: Response of thermohaline circulation to freshwater forcing under present day and LGM conditions. *J. Climate,* **21,** 2239–2258.

Hughes, T. M., and A. J. Weaver, 1994: Multiple equilibria of an asymmetric two-basin ocean model. *J. Phys. Oceanogr.,* **24,** 619–637.

Huisman, S. E., M. Den Toom, H. A. Dijkstra, and S. S. Drijfhout, 2010: An indicator of the multiple equilibria regime of the Atlantic meridional overturning circulation. *J. Phys. Oceanogr.,* **40,** 551–567.

Jahn, A., L. B. Tremblay, R. Newton, M. M. Holland, L. A. Mysak, and I. A. Dmitrenko, 2010: A tracer study of the Arctic Ocean's liquid freshwater export variability. *J. Geophys. Res.,* **115,** C07015, doi:10.1029/2009JC005873.

Killworth, P. D., 1983: Deep convection in the world ocean. *Rev. Geophys. Space Phys.,* **21,** 1–26.

Komuro, Y., and H. Hasumi, 2005: Intensification of the Atlantic deep circulation by the Canadian Archipelago throughflow. *J. Phys. Oceanogr.,* **35,** 775–789.

Lenderink, G., and R. J. Haarsma, 1994: Variability and multiple equilibria of the thermohaline circulation associated with deep water formation. *J. Phys. Oceanogr.,* **24,** 1480–1493.

Liu, Z., and Coauthors, 2009: Transient simulation of last deglaciation with a new mechanism for Bølling-Allerød warming. *Science,* **325,** 310–314.

Manabe, S., and R. J. Stouffer, 1988: Two stable equilibria of a coupled ocean–atmosphere model. *J. Climate,* **1,** 841–866.

Marotzke, J., and J. Willebrand, 1991: Multiple equilibria of the global thermohaline circulation. *J. Phys. Oceanogr.,* **21,** 1372–1385.

——, P. Welander, and J. Willebrand, 1988: Instability and multiple steady states in a meridional-plane model of the thermohaline circulation. *Tellus,* **40A,** 162–172.

Oka, A., and H. Hasumi, 2006: Effects of model resolution on salt transport through northern high-latitude passages and Atlantic meridional overturning circulation. *Ocean Modell.,* **13,** 126–147, doi:10.1016/j.ocemod.2005.12.004.

Power, S., and R. Kleeman, 1993: Multiple equilibria in a global ocean general circulation model. *J. Phys. Oceanogr.,* **23,** 1670–1681.

Rahmstorf, S., 1996: On the freshwater forcing and transport of the Atlantic thermohaline circulation. *Climate Dyn.,* **12,** 799–811.

——, 2002: Ocean circulation and climate changes during the past 120 000 years. *Nature,* **419,** 207–214.

——, and Coauthors, 2005: Thermohaline circulation hysteresis: A model intercomparison. *Geophys. Res. Lett.,* **32,** L23605, doi:10.1029/2005GL023655.

Rennermalm, A. K., E. F. Wood, S. J. Déry, A. J. Weaver, and M. Eby, 2006: Sensitivity of the thermohaline circulation to Arctic Ocean runoff. *Geophys. Res. Lett.,* **33,** L12703, doi:10.1029/2006GL026124.

——, ——, A. J. Weaver, M. Eby, and S. J. Déry, 2007: Relative sensitivity of the Atlantic meridional overturning circulation to river discharge into Hudson Bay and the Arctic Ocean. *J. Geophys. Res.,* **112,** G04S48, doi:10.1029/2006JG000330.

Renold, M., C. C. Raible, M. Yoshimori, and T. F. Stocker, 2010: Simulated resumption of the North Atlantic meridional overturning circulation—Slow basin-wide advection and abrupt local convection. *Quat. Sci. Rev.,* **29,** 101–112, doi:10.1016/j.quascirev.2009.11.005.

Rooth, C., 1982: Hydrology and ocean circulation. *Prog. Oceanogr.,* **11,** 131–149.

Saenko, O. A., A. J. Weaver, and J. M. Gregory, 2003: On the link between the two modes of the ocean thermohaline circulation and the formation of global-scale water masses. *J. Climate,* **16,** 2797–2801.

Schiller, A., U. Mikolajewicz, and R. Voss, 1997: The stability of the North Atlantic thermohaline circulation in a coupled ocean-atmosphere general circulation model. *Climate Dyn.,* **13,** 325–347.

Serreze, M. C., and Coauthors, 2006: The large-scale freshwater cycle of the Arctic. *J. Geophys. Res.,* **111,** C11010, doi:10.1029/2005JC003424.

Sijp, W. P., and M. H. England, 2006: Sensitivity of the Atlantic thermohaline circulation and its stability to basin-scale variations in vertical mixing. *J. Climate,* **19,** 5467–5478.

——, ——, and J. M. Gregory, 2012: Precise calculations of the existence of multiple AMOC equilibria in coupled climate models. Part I: Equilibrium states. *J. Climate,* **25,** 282–298.

Stocker, T. F., and D. G. Wright, 1991a: Rapid transitions of the ocean's deep circulation induced by changes in the surface water fluxes. *Nature,* **351,** 729–732.

——, and ——, 1991b: A zonally averaged ocean model for the thermohaline circulation. Part II: Interocean circulation in the Pacific–Atlantic basin system. *J. Phys. Oceanogr.,* **21,** 1725–1739.

Stommel, H., 1961: Thermohaline convection with two stable regimes of flow. *Tellus,* **2,** 244–230.

Stouffer, R. J., and Coauthors, 2006: Investigating the causes of the response of the thermohaline circulation to past and future climate changes. *J. Climate,* **19,** 1365–1387.

Tziperman, E., J. R. Toggweiler, Y. Feliks, and K. Bryan, 1994: Instability of the thermohaline circulation with respect to mixed boundary conditions: Is it really a problem for realistic models? *J. Phys. Oceanogr.,* **24,** 217–232.

Weaver, A. J., and E. S. Sarachik, 1991: The role of mixed boundary conditions in numerical models of the ocean's climate. *J. Phys. Oceanogr.,* **21,** 1470–1493.

——, and T. M. C. Hughes, 1992: Stability and variability of the thermohaline circulation and its links to climate. *Trends Phys. Oceanogr.,* **1,** 15–70.

——, J. Marotzke, P. F. Cummins, and E. S. Sarachik, 1993: Stability and variability of the thermohaline circulation. *J. Phys. Oceanogr.,* **23,** 39–60.

Weber, S. L., and Coauthors, 2007: The modern and glacial overturning circulation in the Atlantic ocean in PMIP coupled model simulations. *Climate Past,* **3,** 51–64.

Weijer, W., W. P. M. De Ruijter, H. A. Dijkstra, and P. J. Van Leeuwen, 1999: Impact of interbasin exchange on the Atlantic overturning circulation. *J. Phys. Oceanogr.,* **29,** 2266–2284.

Yeager, S. G., C. A. Shields, W. G. Large, and J. J. Hack, 2006: The low-resolution CCSM3. *J. Climate,* **19,** 2545–2566.

Yin, J., and R. J. Stouffer, 2007: Comparison of the stability of the Atlantic thermohaline circulation in two coupled atmosphere–ocean general circulation models. *J. Climate,* **20,** 4293–4315.

Zhang, S., R. J. Greatbatch, and C. A. Lin, 1993: A reexamination of the polar halocline catastrophe and implications for coupled ocean–atmosphere modeling. *J. Phys. Oceanogr.,* **23,** 287–299.